Applied Physics Letters

Determination of band offsets at GaN/single-layer MoS_2 heterojunction

Cite as: Appl. Phys. Lett. **109**, 032104 (2016); https://doi.org/10.1063/1.4959254
Submitted: 21 May 2016 • Accepted: 10 July 2016 • Published Online: 20 July 2016

Malleswararao Tangi, Pawan Mishra, Tien Khee Ng, et al.

Determination of band offsets at GaN/single-layer MoS_2 heterojunction

Malleswararao Tangi,[1,a)] Pawan Mishra,[1,a)] Tien Khee Ng,[1] Mohamed Nejib Hedhili,[2] Bilal Janjua,[1] Mohd Sharizal Alias,[1] Dalaver H. Anjum,[2] Chien-Chih Tseng,[3] Yumeng Shi,[3] Hannah J. Joyce,[4] Lain-Jong Li,[3] and Boon S. Ooi[1,b)]

[1]*Photonics Laboratory, King Abdullah University of Science and Technology (KAUST), Thuwal 23955-6900, Saudi Arabia*

[2]*Adavanced Nanofabrication Imaging and Characterization, King Abdullah University of Science and Technology (KAUST), Thuwal 23955-6900, Saudi Arabia*

[3]*Physical Sciences and Engineering Division, King Abdullah University of Science and Technology (KAUST), Thuwal 23955-6900, Saudi Arabia*

[4]*Department of Engineering, University of Cambridge, 9 JJ Thomson Avenue, Cambridge, Cambridgeshire CB3 0FA, United Kingdom*

(Received 21 May 2016; accepted 10 July 2016; published online 20 July 2016; corrected 25 July 2016)

We report the band alignment parameters of the GaN/single-layer (SL) MoS_2 heterostructure where the GaN thin layer is grown by molecular beam epitaxy on CVD deposited SL-MoS_2/c-sapphire. We confirm that the MoS_2 is an SL by measuring the separation and position of room temperature micro-Raman E^1_{2g} and A^1_g modes, absorbance, and micro-photoluminescence bandgap studies. This is in good agreement with HRTEM cross-sectional analysis. The determination of band offset parameters at the GaN/SL-MoS_2 heterojunction is carried out by high-resolution X-ray photoelectron spectroscopy accompanying with electronic bandgap values of SL-MoS_2 and GaN. The valence band and conduction band offset values are, respectively, measured to be 1.86 ± 0.08 and 0.56 ± 0.1 eV with type II band alignment. The determination of these unprecedented band offset parameters opens up a way to integrate 3D group III nitride materials with 2D transition metal dichalcogenide layers for designing and modeling of their heterojunction based electronic and photonic devices.
[http://dx.doi.org/10.1063/1.4959254]

Regardless of the large number of defects, GaN remains as a potential semiconducting material with enormous applications in high efficiency electronic and optoelectronics devices, such as high electron mobility transistors, light emitting diodes, and laser diodes.[1–4] These unavoidable defects in GaN mainly stem from its large lattice mismatch with the most commonly used foreign substrates Sapphire, SiC, and Si.[5,6] On the other hand, transition metal dichalcogenides (TMDs) are emerging as a novel material system exhibiting good electronic and optoelectronic properties in recent years.[7–9] Recently it has been reported[10] that GaN exhibits small lattice mismatch (≈0.8%) with respect to molybdenum disulfide (MoS_2) which is a widely studied and well understood atomic layered material that pertains to the family of TMDs. In literature, there were limited efforts on growing this technologically important direct bandgap GaN material on lattice matched MoS_2 exhibiting indirect bandgap with multiple layers. For instance, the first report by Yamada *et al.* has demonstrated the growth of GaN on bulk MoS_2 by molecular beam epitaxy (MBE).[11] There were recent attempts to grow GaN on MoS_2 flakes[10] and layered MoS_2 on GaN epilayers[12] by chemical vapor deposition (CVD) growth techniques. Though the deposition of large area (up to 1 cm^2) single-layer (SL) MoS_2 on sapphire exhibiting direct bandgap is achievable,[13] the growth of GaN on such large area MoS_2 monolayers has not yet been explored.

Of late, most of the researchers studied the band offset parameters for either group III nitrides on various other semiconducting materials or solely TMDs based dissimilar heterostructures by using photoemission core-levels measured with respect to the valence band spectra and bandgap studies. However, band offset parameters (Junction type: valence band offset (VBO)—ΔE_v and conduction band offset (CBO)—ΔE_c) are measured for various heterojunctions in the literature, such as InN/GaN (Type-I: 0.58 ± 0.08 and 2.22 ± 0.1 eV),[14] GaN/AlN (Type-I: 0.8 ± 0.3 and ≈1.6 eV),[15] InN/AlN (Type-I: 1.52 ± 0.17 and 4.00 ± 0.2 eV),[16] InN/p-Si (Type-III: 1.39 and 1.81 eV),[17] ZnO/GaN (Type-II: 0.7 and 0.8 eV),[18] and MoS_2/WSe_2 (Type-II: 0.83 and 0.76 eV).[19] To date there is no experimental report on the determination of band offset parameters (ΔE_v and ΔE_c) and type of heterojunction by high-resolution X-ray photoelectron spectroscopy (HRXPS) for epitaxially formed GaN/SL-MoS_2 heterojunction. This determination plays a crucial role to evolve the electron transport properties of future devices consisting of this heterojunction. Thus, the growth of GaN/SL-MoS_2 and the study of band offsets open up a way to integrate group III nitrides (3D layers) with TMDs (2D layers) for designing and modeling of their heterojunction based electronic and photonic devices.

In the present work, in order to study the band alignment at the heterojunction formed by GaN/SL-MoS_2, epitaxial GaN layers were grown on CVD prepared SL-MoS_2. Then the optical properties of GaN epitaxial layers and

[a)]M. Tangi and P. Mishra contributed equally to this work.
[b)]Author to whom correspondence should be addressed. Electronic mail: boon.ooi@kaust.edu.sa

MoS_2/c-sapphire substrates were studied by means of Raman and micro-photoluminescence (μPL) spectroscopic measurements, which confirmed sustainability of SL-MoS_2 at GaN growth temperature, in agreement with HRTEM cross-section analysis. Further, the band offset parameters of GaN/SL-MoS_2 heterojunction were determined using high-resolution X-ray photoelectron spectroscopy (HRXPS) and micro-photoluminescence (μPL) measurements.

MoS_2 SLs were deposited on c-sapphire substrates using CVD and the details are published elsewhere.[20] Further, the growth experiments of GaN on MoS_2/c-sapphire substrates were performed by Veeco 930 Gen radio frequency-plasma assisted molecular beam epitaxy (RF-PAMBE) system at substrate temperature of 500 °C. The ion and a cryo pumps were used to achieve a base pressure of 3×10^{-11} Torr and oxygen partial pressure $<10^{-12}$ Torr, as determined by a residual gas analyzer (RGA). The substrates were thermally degassed in introduction chamber at 200 °C for 30 min, and further cleaning was carried out in a preparation chamber at 300 °C for 60 min and in the growth chamber at 400 °C for 30 min. While preparing the substrate in the growth temperature, the degradation of MoS_2 was monitored by *in-situ* reflection high-energy electron diffraction (RHEED). For GaN growth, the nitrogen plasma source was operated with the flow rate of 1 standard cubic centimeter per minute (sccm) and RF power of 300 W and Ga metal was evaporated by standard Knudsen cell with beam equivalent pressure (BEP) value of 2.10×10^{-8} Torr. The corresponding chamber pressure was $\approx 2.5 \times 10^{-5}$ Torr. The thickness of the GaN epilayer (sample C) is measured by Profilometer and is found to be ≈500 nm. Transmission Electron Microscopy (TEM) studies were carried out using Titan with electron beam energy of 400 keV. The band edge emission of GaN and MoS_2 samples were obtained using Aramis room temperature micro-photoluminescence (μPL) with excitation lines as He-Cd laser of 325 nm and Cobalt laser of 473 nm having objective lenses of 40× and 100×, respectively. The Cobalt laser was used for micro-Raman measurements. The high-resolution XPS measurements were carried out using a Kratos Axis Ultra DLD spectrometer equipped with a monochromatic Al K_α X-ray source ($h\nu = 1486.6$ eV) operating at 150 W, a multi-channel plate, and delay line detector under a vacuum of $\sim 10^{-9}$ mbar. The instrumental resolution is 0.45 eV. All spectra were recorded using an aperture slot of $\approx 300\,\mu m^2$. The high-resolution spectra were collected at fixed analyzer pass energy of 20 eV. A clean copper (Cu) foil was electrically connected to the sample surface so as to compensate the photoemission induced positive charge shifts. Further, binding energies were referenced to the adventitious carbon signal. The peak deconvolution was accomplished by CasaXPS software. In this study, CVD grown SL-MoS_2 (sample A), MBE grown GaN on SL-MoS_2 (sample B), and GaN epilayer (sample C) were used to determine the band offsets at GaN/SL-MoS_2 heterostructure. The thickness of GaN layer in sample B was estimated to be 3 ± 1 nm from growth rate calibrations.

In order to assure that the CVD grown MoS_2 consists of single layer in samples (A and B) and the quality of epitaxial GaN (in samples B and C), micro-Raman spectroscopic measurements were carried out. Figs. 1(a)–1(c) show the Raman spectra for MoS_2/c-sapphire, GaN/MoS_2/c-sapphire, and GaN/c-sapphire. Figs. 1(a) and 1(b) show the E^1_{2g} and A^1_g phonon modes at 385.5 ± 0.5 and $405.0 \pm 0.5\,cm^{-1}$, which correspond to the in plane vibration of Mo and S atoms (E^1_{2g}) and out of plane vibration of S atoms (A^1_g) in MoS_2, respectively. The low intensity broad peak at $\approx 465\,cm^{-1}$ in Figs. 1(a) and 1(b) represents 2LA mode.[21] The separation between E^1_{2g} and A^1_g phonon modes is observed to be $19.5 \pm 0.5\,cm^{-1}$, which confirms that the MoS_2 on c-sapphire deposited by CVD is a single-layer.[22–24] The intensity ratio (I_A/I_E) of A^1_g and E^1_{2g} modes decreases from sample A to B which could be due to the unintentional doping of MoS_2 monolayer in sample B.[25] This doping may arise from the exposure to nitrogen plasma during the growth of GaN on SL-MoS_2 in UHV-MBE environment. In addition to these MoS_2 phonon modes, sample B consists of low intense E^H_2 phonon characteristic for 3 nm thick GaN layer grown on SL-MoS_2. In Fig. 1(b), the observed weak signal of E^H_2 mode in comparison with A^1_g and E^1_{2g} modes is a consequence of the reduced resonant excitation effect as the band-edge emission of GaN is higher than the excitation line ($E_g^{GaN} > E_{exc}$). Thereby, Fig. 1(b) concludes the sustainability of SL-MoS_2 during the epitaxial growth of GaN. Fig. 1(c) shows the Raman spectra acquired on GaN epi-film having E^H_2 phonon mode at $568.5 \pm 0.5\,cm^{-1}$ which matches with the E^H_2 phonon mode of GaN thin layer in sample B. This infers that GaN thin layer in sample B is as relaxed as that in sample C which is due to the less lattice mismatch (0.8%) between GaN and SL-MoS_2. The inset represents the cross-sectional HRTEM image acquired at the typical GaN/SL-MoS_2/c-sapphire heterojunction having thickness of MoS_2 ≈0.8 nm, which is in agreement with the thickness of S-Mo-S single-layer. Thus, micro-Raman and HRTEM measurements confirm the existence of single layered MoS_2 during the growth of relaxed GaN.

Optical quality of both MoS_2 and bulk like GaN epilayer (samples A and C) are verified by room temperature μPL measurements. Fig. 2 shows the RT μPL and optical absorbance spectra obtained on sample A and the respective inset

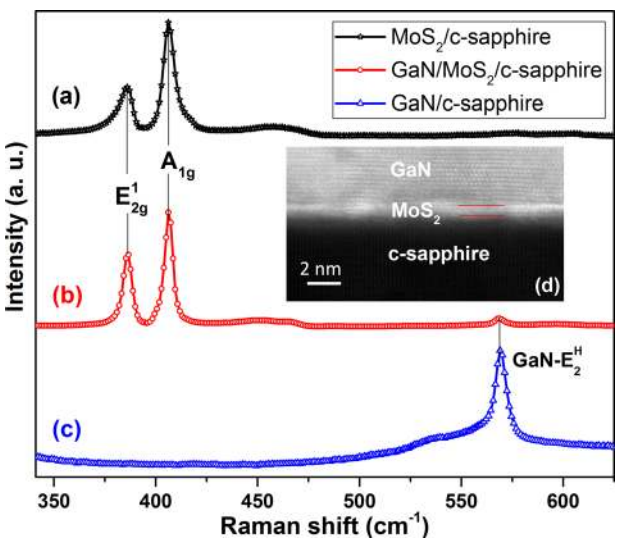

FIG. 1. (a)–(c) The micro-Raman spectra of samples A–C acquired on MoS_2, GaN/MoS_2, and epi-GaN samples, respectively. The inset (d) shows the HRTEM cross-sectional image obtained at a typical GaN/SL-MoS_2/c-sapphire heterojunction.

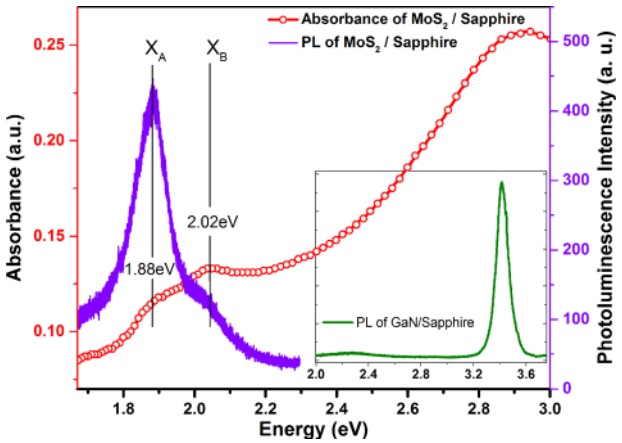

FIG. 2. The micro-photoluminescence (right y-axis) and absorbance spectra (left y-axis) of MoS_2. The inset is micro-photoluminescence spectrum for GaN epilayer.

shows the μPL band edge emission for sample C. As represented in Fig. 2, the observed states X_A and X_B at 1.88 and 2.02 eV in absorbance and μPL spectra are the exciton resonances corresponding to the transitions from broken inversion symmetry induced two spin-split valence sub-bands to the conduction band and vice versa.[9,26,27] This observation confirms that the CVD grown MoS_2 sample is in the form of single-layer, as corroborated by earlier micro Raman and HRTEM measurements, exhibiting the direct optical bandgap ($E_{opt}^{MoS_2}$) value of ≈1.88 eV. The inset of Fig. 2 shows the optical band edge emission for GaN (E_{opt}^{GaN}) at ≈3.43 eV. However, these are not exact band to band transitions due to the involvement of excitons. The electronic band gap is a measure of actual gap of a material which is the summation of optical bandgap and exciton (electron-hole) binding energy ($E_g = E_{opt} + E_b$).[28] Hence, these observed optical bandgap values differ from reported electronic bandgap values of $E_g^{SL\text{-}MoS_2} = 2.15$ eV and $E_g^{GaN} = 3.45$ eV by their respective exciton binding energy (E_b) values of ≈0.220 eV and ≈0.023 eV in the literature.[19,29,30]

High-resolution XPS measurements are direct, most reliable, and extensively employed to determine the valence band offset (VBO) of a heterojunction interface. In order to evaluate VBO at GaN/SL-MoS_2 heterointerface, the energy difference between the Ga and Mo core levels from the GaN/SL-MoS_2 heterojunction sample and the energy of core levels relative to the respective valence band maximum of the GaN epilayer and SL-MoS_2 samples need to be acquired. Since the escape depth of photo emitted electrons in HRXPS is remarkably low, over grown GaN layer of heterojunction sample has to be thin enough in such a way that the electrons knocked out from both thin overgrown GaN and underlying SL-MoS_2 layers can be easily probed.[31] As the SL-MoS_2 is not formed continuously on the entire Sapphire substrate, the region of interest on GaN/MoS_2 and MoS_2/Sapphire samples was selectively chosen within the spatial resolution of HRXPS measurements by comparing the intensity of Ga 2p, Mo 3d, and Al 2p core-levels. This allowed us to collect the photoemission signal from solely SL-MoS_2/Sapphire and GaN/SL-MoS_2 heterostructures for samples A and B, respectively. The valence band offset (VBO) for GaN/SL-MoS_2 heterojunction can be calculated by the method provided by Kraut *et al.*,[32] expressed as

$$\Delta E_v = \Delta E^{MoS_2}_{Mo3d_{5/2}-VBM} + \Delta E^{GaN/MoS_2}_{Ga2p_{3/2}-Mo3d_{5/2}} - \Delta E^{GaN}_{Ga2p_{3/2}-VBM}, \quad (1)$$

where the first term on right side of Equation (1) is the core-level energy of $Mo3d_{5/2}$ determined with respect to the valence band maximum for SL-MoS_2. Fig. 3(a-i) shows the Mo 3d and S 2s core-level spectra collected from SL-MoS_2 which can be deconvoluted using Voigt line shapes, with Mo-S and S-Mo chemical states. Additionally, Mo 3d has low intensity chemical state at 232.54 eV which corresponds to Mo-O chemical state that results from MoO_3 precursor or excess Mo metal bonding with oxygen of c-Al_2O_3 at the interface of MoS_2/c-sapphire during high temperature CVD growth. Fig. 3(a-ii) shows VB spectra where the valence band maxima of the samples are obtained by extrapolating linear leading edge to the base line of respective valence band photoelectron spectrum. This VBM is measured to be 1.00 ± 0.08 eV as depicted in Fig. 3(a-ii). Thereby, the separation between the core-level energy of $Mo3d_{5/2}$ and valence band maximum ($\Delta E^{MoS_2}_{Mo3d_{5/2}-VBM} = E^{MoS_2}_{Mo3d_{5/2}} - E^{MoS_2}_{VBM}$) for SL-$MoS_2$ is determined to be 228.60 ± 0.08 eV as described in Fig. 3(a).

The subsequent term in Eq. (1) represents the core-level difference that is measured from the photoelectron spectrum of heterojunction sample GaN/SL-MoS_2. Figs. 3(b-i) and 3(b-ii) show the Ga 2p and Mo 3d core-levels which result from the GaN/SL-MoS_2, respectively. Fig. 3(b-i) is the Ga 2p core-level spectrum which is fitted by solely Ga-N bonding. Fig. 3(b-ii) shows that the deconvoluted Mo 3d core-level spectrum establishes three Mo $3d_{5/2}$ chemical states at 229.31 ± 0.08, ≈227.97 ± 0.08, and 232.95 ± 0.08 eV, assigned to the Mo-S in 2H-MoS_2 (trigonal prismatic), Mo-S in 1T-MoS_2 (octahedral), and Mo-O in MoO_3, respectively. The Mo $3d_{3/2}$ core-level has similar deconvolutions at higher binding energy values differing with ≈3.16 eV for these chemical states. The presence of octahedral phase could be due to the unintentional N-plasma intercalation of MoS_2 layer during GaN growth which is as similar as the reported Lithium intercalation.[9] The peak at 226.59 ± 0.08 eV corresponds to the S 2s core-level which indicates S-Mo bonding. The S 2s core levels in Figs. 3(a-ii) and 3(b-i) are fitted with similar peaks having same fitting parameters. Extremely high intensity of Mo-S peak infers the sustainability of SL-MoS_2 at GaN growth temperature under UHV oxygen free conditions. The absence of any other chemical state associated with Mo or S in Ga 2p core-level spectrum is a clear evidence of Van der Waal epitaxy. The energy difference ($\Delta E^{GaN/MoS_2}_{Ga2p_{3/2}-Mo3d_{5/2}} = E^{GaN/MoS_2}_{Ga2p_{3/2}} - E^{GaN/MoS_2}_{Mo3d_{5/2}}$) between Mo $3d_{5/2}$ and Ga $2p_{3/2}$ core-levels is observed to be 888.50 ± 0.08 eV.

The last term indicates the core-level energy (1115.23 ± 0.08 eV) of $Ga2p_{3/2}$ measured relative to the respective VBM of 2.27 ± 0.08 eV ($\Delta E^{GaN}_{Ga2p_{3/2}-VBM} = E^{GaN}_{Ga2p_{3/2}} - E^{GaN}_{VBM}$) as described in Fig. 3(c). In Fig. 3(c-i), Ga $2p_{5/2}$ and Ga $2p_{3/2}$ core-level is deconvoluted with Ga-N bonding state at 1117.50 ± 0.08 and 1144.40 ± 0.08 eV. The observed broad

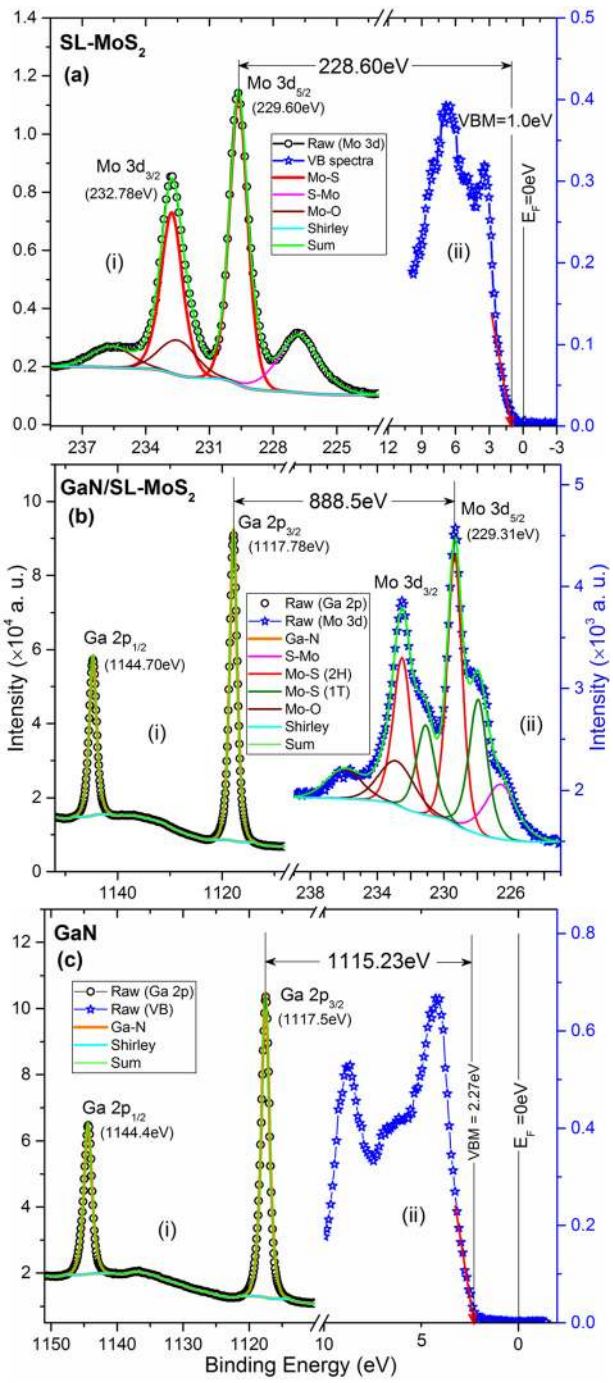

FIG. 3. (a-i) and (a-ii) The Mo 3d core-level and valence band spectra of single-layer MoS_2. (b-i) and (b-ii) Ga 2p core-level and Mo 3d spectra of GaN/SL-MoS_2. (c-i) and (c-ii) Ga 2p core-level and valence band spectra acquired on GaN epilayer. The peak positions of core-levels are given in parentheses.

tails at ≈1135 eV in Figs. 3(b-i) and 3(c-i) are due to the inelastic scattering loss of electrons (satellite peaks) in GaN. The Fermi level position with respect to the VBM, as shown in Figs. 3(a-ii) and 3(c-ii), infers that the GaN epilayer and SL-MoS_2 are nearly intrinsic materials. The Mo 3p, 4p, and Ga 3d core-level peaks have not been considered in the analysis since these levels closely merge with N-like s levels at the bottom of the valence band. In such a case, the s-like contribution cannot be easily distinguished from the p- or d-like contribution as the peak fitting cannot be accomplished with the same symmetric Voigt functions, and thus these core-levels are not useful in determining band offsets.

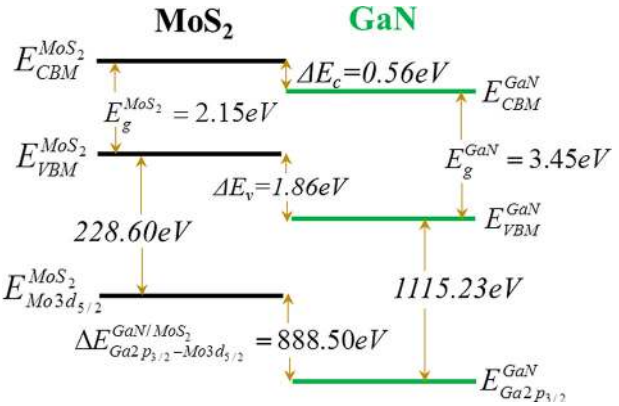

FIG. 4. The schematic representation of band alignment at GaN/SL-MoS_2 heterojunction.

Thereby substitution of VBO (ΔE_v) obtained from HRXPS analysis (Fig. 3) and electronic bandgap (E_g) values of SL-MoS_2 and GaN epilayer in the following equation allows to measure the conduction band offset (CBO) ΔE_c for GaN/SL-MoS_2 heterostructure:

$$\Delta E_c = E_g^{MoS_2} + \Delta E_v - E_g^{GaN}. \quad (2)$$

Hence, measured CBO (ΔE_c) is 0.56 ± 0.1 eV which renders a less potential barrier height and favors good electron transport properties across the junction. This value for nearly intrinsic epitaxial-GaN/SL-MoS_2 junction in present study is higher than recently reported CBO value (0.23 eV) for layer transferred p-MoS_2/n-GaN diode.[33] Thus, the experimentally determined offset parameters from this study are represented as a schematic of band alignment diagram in Fig. 4 which infers that this band alignment pertains to type-II heterostructure.

In summary, GaN epitaxial layers were deposited on SL-MoS_2/c-sapphire substrates by molecular beam epitaxy to study band alignment of the GaN/SL-MoS_2 heterostructure. We confirm that deposited MoS_2 is a single-layer by measuring the separation and position of micro-Raman modes, absorbance, and photoluminescence studies. This is further verified by HRTEM cross-section analysis. The determination of band offset parameters at GaN/SL-MoS_2 heterostructure is carried out by using high-resolution X-ray photoelectron and micro-photoluminescence spectroscopies. We determine a valence band offset value of 1.86 ± 0.08 eV and conduction band offset of 0.56 ± 0.1 eV with type II band alignment at GaN/SL-MoS_2 heterostructure. This determination of unprecedented band offset parameters opens up a way to integrate 3D group III nitride materials with 2D transition metal dichalcogenide layers.

We acknowledge the financial support from King Abdulaziz City for Science and Technology (KACST) Grant No. KACST TIC R2-FP-008 and baseline funding BAS/1/1614-01-01 of the King Abdullah University of Science and Technology (KAUST).

[1]S. Nakamura, Science **281**, 956 (1998).
[2]S. Nakamura, Annu. Rev. Mater. Sci. **28**, 125 (1998).
[3]U. K. Mishra, P. Parikh, and Y.-F. Wu, Proc. IEEE **90**, 1022 (2002).

[4]C. Zhao, T. K. Ng, N. Wei, A. Prabaswara, M. S. Alias, B. Janjua, C. Shen, and B. S. Ooi, Nano Lett. **16**, 1056 (2016).
[5]M. A. Reshchikov and H. Morkoç, J. Appl. Phys. **97**, 061301 (2005).
[6]L. Liu and J. H. Edgar, Mater. Sci. Eng. R Rep. **37**, 61 (2002).
[7]B. Radisavljevic, A. Radenovic, J. Brivio, V. Giacometti, and A. Kis, Nat. Nanotechnol. **6**, 147 (2011).
[8]B. W. H. Baugher, H. O. H. Churchill, Y. Yang, and P. Jarillo-Herrero, Nat. Nanotechnol. **9**, 262 (2014).
[9]G. Eda, H. Yamaguchi, D. Voiry, T. Fujita, M. Chen, and M. Chhowalla, Nano Lett. **11**, 5111 (2011).
[10]P. Gupta, A. A. Rahman, S. Subramanian, S. Gupta, A. Thamizhavel, T. Orlova, S. Rouvimov, S. Vishwanath, V. Protasenko, M. R. Laskar, H. G. Xing, D. Jena, and A. Bhattacharya, Sci. Rep. **6**, 23708 (2016).
[11]A. Yamada, K. P. Ho, T. Maruyama, and K. Akimoto, Appl. Phys. A Mater. Sci. Process. **69**, 89 (1999).
[12]D. Ruzmetov, K. Zhang, G. Stan, B. Kalanyan, G. R. Bhimanapati, S. M. Eichfeld, R. A. Burke, P. B. Shah, T. P. O'Regan, F. J. Crowne, A. G. Birdwell, J. A. Robinson, A. V. Davydov, and T. G. Ivanov, ACS Nano **10**, 3580 (2016).
[13]D. Dumcenco, D. Ovchinnikov, K. Marinov, P. Lazić, M. Gibertini, N. Marzari, O. L. Sanchez, Y.-C. Kung, D. Krasnozhon, M.-W. Chen, S. Bertolazzi, P. Gillet, A. Fontcuberta i Morral, A. Radenovic, and A. Kis, ACS Nano **9**, 4611 (2015).
[14]P. D. C. King, T. D. Veal, C. Kendrick, L. Bailey, S. Durbin, and C. F. McConville, Phys. Rev. B **78**, 033308 (2008).
[15]G. Martin, S. Strite, A. Botchkarev, A. Agarwal, A. Rockett, H. Morkoç, W. R. L. Lambrecht, and B. Segall, Appl. Phys. Lett. **65**, 610 (1994).
[16]P. D. C. King, T. D. Veal, P. H. Jefferson, C. F. McConville, P. J. Parbrook, and H. Lu, Appl. Phys. Lett. **90**, 132105 (2007).
[17]T. N. Bhat, M. Kumar, M. K. Rajpalke, B. Roul, S. B. Krupanidhi, and N. Sinha, J. Appl. Phys. **109**, 123707 (2011).
[18]J. W. Liu, A. Kobayashi, S. Toyoda, H. Kamada, A. Kikuchi, J. Ohta, H. Fujioka, H. Kumigashira, and M. Oshima, Phys. Status Solidi Basic Res. **248**, 956 (2011).
[19]M.-H. Chiu, C. Zhang, H.-W. Shiu, C.-P. Chuu, C.-H. Chen, C.-Y. S. Chang, C.-H. Chen, M.-Y. Chou, C.-K. Shih, and L.-J. Li, Nat. Commun. **6**, 7666 (2015).
[20]Y. H. Lee, X. Q. Zhang, W. Zhang, M. T. Chang, C. Te Lin, K. Di Chang, Y. C. Yu, J. T. W. Wang, C. S. Chang, L. J. Li, and T. W. Lin, Adv. Mater. **24**, 2320 (2012).
[21]J.-U. Lee, K. Kim, S. Han, G. H. Ryu, Z. Lee, and H. Cheong, ACS Nano **10**, 1948 (2016).
[22]H. Liu and D. Chi, Sci. Rep. **5**, 11756 (2015).
[23]C. Lee, H. Yan, L. E. Brus, T. F. Heinz, J. Hone, and S. Ryu, ACS Nano **4**, 2695 (2010).
[24]V. Kranthi Kumar, S. Dhar, T. H. Choudhury, S. A. Shivashankar, and S. Raghavan, Nanoscale **7**, 7802 (2015).
[25]B. Chakraborty, A. Bera, D. V. S. Muthu, S. Bhowmick, U. V. Waghmare, and A. K. Sood, Phys. Rev. B **85**, 161403(R) (2012).
[26]K. F. Mak and J. Shan, Nat. Photonics **10**, 216 (2016).
[27]W. Jin, P. C. Yeh, N. Zaki, D. Zhang, J. T. Sadowski, A. Al-Mahboob, A. M. Van Der Zande, D. A. Chenet, J. I. Dadap, I. P. Herman, P. Sutter, J. Hone, and R. M. Osgood, Phys. Rev. Lett. **111**, 106801 (2013).
[28]M. M. Ugeda, A. J. Bradley, S.-F. Shi, F. H. da Jornada, Y. Zhang, D. Y. Qiu, W. Ruan, S.-K. Mo, Z. Hussain, Z.-X. Shen, F. Wang, S. G. Louie, and M. F. Crommie, Nat. Mater. **13**, 1091 (2014).
[29]S. Q. Zhou, M. F. Wu, L. N. Hou, S. D. Yao, H. J. Ma, R. Nie, Y. Z. Tong, Z. J. Yang, T. J. Yu, and G. Y. Zhang, J. Cryst. Growth **263**, 35 (2004).
[30]J. F. Muth, J. H. Lee, I. K. Shmagin, R. M. Kolbas, H. C. Casey, B. P. Keller, U. K. Mishra, and S. P. DenBaars, Appl. Phys. Lett. **71**, 2572 (1997).
[31]C. S. Fadley, Surf. Interface Anal. **40**, 1579 (2008).
[32]E. A. Kraut, R. W. Grant, J. R. Waldrop, and S. P. Kowalczyk, Phys. Rev. Lett. **44**, 1620 (1980).
[33]E. W. Lee II, C. H. Lee, P. K. Paul, L. Ma, W. D. McCulloch, S. Krishnamoorthy, Y. Wu, A. R. Arehart, and S. Rajan, Appl. Phys. Lett. **107**, 103505 (2015).